ELSEVIER

International Journal of Heat and Fluid Flow 21 (2000) 197–206

International Journal of HEAT AND FLUID FLOW

www.elsevier.com/locate/ijhff

Finite element analysis of incompressible viscous flow with moving free surface by selective volume of fluid method

Suho Shin [a], Woo Il Lee [b,*]

[a] *Opto-mechatronics Laboratory, Samsung Electronics, Suwon, Kyungki-Do 442-742, South Korea*
[b] *Department of Mechanical Engineering, Seoul National University, Seoul 151-742, South Korea*

Received 2 November 1998; accepted 26 October 1999

Abstract

A numerical technique for simulating incompressible viscous flow with free surface is presented. The flow field was calculated by the penalty finite element formulation. In this work, a modified volume of fluid (VOF) method based on four node elements in 2D geometry was proposed for its compatibility with the irregular meshes generally used with the finite element method (FEM). Numerical analyses were done for two benchmark examples, namely the broken dam problem and the solitary wave propagation problem. The numerical results showed close agreement with the existing data. In order to demonstrate the effectiveness of the proposed numerical scheme, mold filling process was studied.

Keywords: Moving free surface; Volume of fluid (VOF) method; Finite element method; Selective VOF method; Mold filling

Notation

c	average velocity of wave
d	depth
F	volume fraction of fluid
F_Γ	fraction of actual fluid volume transferred through boundary of an element
$\boldsymbol{f}$	body force vector
g	gravity
H	initial height of fluid column or wave
H_e	element characteristic length
L	length
$\boldsymbol{n}$	outward unit normal vector
P	pressure
R_{max}	maximum run-up height of wave
t	time
$\boldsymbol{u}$	velocity vector
$\hat{\boldsymbol{u}}$	velocity vector at previous iteration
u_e	velocity at element center
u_i	ith component of the velocity vector
$\hat{u}_i$	ith component of the velocity vector at previous iteration
V_k^i	volume of the kth sub-element in the ith control volume
$\boldsymbol{w}$	Galerkin weighting function
$\tilde{\boldsymbol{w}}$	modified weighting function added by the streamline upwind contribution
$\boldsymbol{x}$	vector
x, y	components in Cartesian coordinate

Greeks

α	element Reynolds number
Γ	boundary
γ	penalty parameter
η	initial wave elevation function
μ	viscosity
ρ	density
τ	viscous stress
Ω	domain

Superscripts

old	previous time step
new	present time step
*	designates non-dimensionalized parameters

Subscripts

A	acceptor
CV	control volume
D	donor
DD	neighboring element of a donor placed opposite to the acceptor
DS1, DS2	neighboring elements of a donor

1. Introduction

Incompressible viscous flow with moving free surface is an engineering problem with many practical aspects. The applications may include materials processing such as, for example, metal casting or injection and compression moldings of polymers. In these applications, flows with moving boundaries are encountered in mold filling processes and are affected by many factors such as material properties, mold geometry and process conditions.

* Corresponding author.
E-mail address: wilee@snu.ac.kr (W.I. Lee).

0142-727X/00/$ - see front matter
PII: S0142-727X(99)00083-1

The most important task in the analysis of flow with moving free surface is determination of the location of the moving free surface. Methods employed to solve such problems can be classified into two groups; Lagrangian and Eulerian schemes (Floryan and Rasmussen, 1989). The former scheme employs a moving grid system, in which each computational mesh is moved or deformed as the free surface advances. The Eulerian method uses a fixed grid system which is generated over the entire domain and is not changed until the completion of calculation. The scheme should be selected considering the strengths and limitations of the algorithms together with the characteristics of the problem.

Lagrangian scheme (Bellet and Chenot, 1993) is characterized by the mesh system which is moved or deformed as the calculation proceeds. The mesh boundaries coincide with the free surface, and thus the free surface can be represented with accuracy. However, overly distorted meshes due to the change of fluid domain may result in numerical errors. The Arbitrary Lagrangian Eulerian (ALE) method (Ramaswamy and Kawahara, 1987; Huerta and Liu, 1988; Choi, 1996), which allows continuous reasoning, has a similar limitation.

In Eulerian schemes, computational meshes are generated beforehand and fixed during entire computation. Therefore, it is free from difficulties due to the deforming meshes. However, a special treatment is necessary to track the moving free surface because the motion of fluid does not coincide with the calculation mesh. MAC method (Harlow and Welch, 1965; Viecelli, 1969; Chan and Street, 1970) follows the moving free surface by tracking the movement of imaginary markers. VOF method, introduced by Hirt and Nichols (1981), is popular in flow problems with moving free surface. In this method, whole domain is divided into cells or control volumes and the volume fraction of fluid in each cell is defined. The flow front is advanced by solving the following transport equation of the fluid:

$$\frac{\partial F}{\partial t} + \boldsymbol{u} \cdot \nabla F = 0. \tag{1}$$

Here F is the volume fraction of the fluid in a cell and $\boldsymbol{u}$ is the flow velocity vector. Even though an additional equation must be solved, overall computation time is usually shorter due to the fixed grid system. Since VOF method represents the shape of the free surface in a relatively simple way, it can be easily applied to existing numerical codes with various numerical schemes (Nichols et al., 1980; Partom, 1987; Lin and Hwang, 1988; Dhatt et al., 1990; Usmani et al., 1992; Swaminathan and Voller, 1994; Rice, 1993; Lewis et al., 1995; Tezduyar et al., 1998).

In this study, a computer code based on the finite element method and the VOF method was developed to trace the moving free surface of the incompressible viscous flow. A "selective" VOF method which is compatible with four node element in two-dimensional flow was proposed to improve the previous donor acceptor scheme. In the proposed scheme, the volume flux of fluid across the element boundary is calculated by using the volume fraction of element only without complicated algorithm or additional mesh system. Therefore, this scheme can be applied to irregular mesh system, and can be easily extended to three-dimensional geometry.

2. Governing equations and finite element formulation

Consider incompressible laminar, Newtonian two-dimensional flow with constant properties. The flow may have a free boundary which is not fixed in space and changes with time. The problem at hand is to obtain the velocity and the pressure distributions as well as the free surface location as functions of time. The governing equations, i.e., the continuity and momentum conservation equations, can be written as

$$\nabla \cdot \boldsymbol{u} = 0, \tag{2}$$

$$\rho\left(\frac{\partial \boldsymbol{u}}{\partial t} + \boldsymbol{u} \cdot \nabla \boldsymbol{u}\right) = -\nabla P + \nabla \cdot \tau + \boldsymbol{f}, \tag{3}$$

$$\tau = \mu\left(\nabla \boldsymbol{u} + \nabla^{\mathrm{T}} \boldsymbol{u}\right), \tag{4}$$

where τ is the viscous stress, P the pressure, $\boldsymbol{f}$ the body force and μ the viscosity of fluid.

The initial and boundary conditions can be stated as (see Fig. 1)

$$\text{initial condition}: \quad \boldsymbol{u} = \boldsymbol{u}(\boldsymbol{x}, 0), \tag{5}$$

$$\text{boundary condition}: \quad \boldsymbol{u} = \boldsymbol{u}(\boldsymbol{x}, t) \quad \text{on } \Gamma_1, \tag{6a}$$

$$(-P\boldsymbol{I} + \tau) \cdot \boldsymbol{n} = \bar{\sigma} \quad \text{on } \Gamma_2, \tag{6b}$$

where $\boldsymbol{n}$ is the unit vector outward normal to the free surface. Γ_1 denotes the boundary where the flow velocity is given. Free surface is represented by Γ_2 along which the normal stress to the free surface $\bar{\sigma}$ is specified.

In this work, the finite element method was used for solving the governing equations. In order to incorporate the continuity equation (Eq. (2)), the penalty formulation (Hughes et al., 1979; Reddy and Gartling, 1994; Carey and Oden, 1986) was adopted. The pressure term in the momentum conservation equation (Eq. (3)) is thus replaced by

$$P = -\gamma \nabla \cdot \boldsymbol{u}, \tag{7}$$

where γ is the penalty parameter. γ is taken as an arbitrary large number ($O(10^4$–$10^{13})$) depending on the Reynolds number and viscosity (Hughes et al., 1979).

The momentum conservation equations were integrated in time using the implicit method. Picard iteration known as successive substitution was used to linearize convection terms. In order to prevent wiggles which may appear in convection dominated problems, streamlines-upwind/Petrov–Galerkin (SU/PG) method (Brooks and Hughes, 1982) was applied to handle the convection terms.

After some straightforward manipulation, the weak formulation for governing equations can be derived as (Hughes et al., 1979)

$$\int_\Omega \rho \frac{\partial \boldsymbol{u}}{\partial t} \cdot \boldsymbol{w}\,\mathrm{d}\Omega + \int_\Omega \rho\left(\hat{\boldsymbol{u}} \cdot \nabla\right)\boldsymbol{u} \cdot \tilde{\boldsymbol{w}}\,\mathrm{d}\Omega + \int_\Omega (\mu \nabla \boldsymbol{u} : \nabla \boldsymbol{w} + \gamma(\nabla \cdot \boldsymbol{u})(\nabla \cdot \boldsymbol{w}))\,\mathrm{d}\Omega = \int_\Omega \boldsymbol{f} \cdot \boldsymbol{w}\,\mathrm{d}\Omega + \int_\Gamma \bar{\sigma} \cdot \boldsymbol{w}\,\mathrm{d}\Gamma, \tag{8}$$

where $\hat{\boldsymbol{u}}$ is the velocity at previous iteration, $\boldsymbol{w}$ the Galerkin weighting function and $\tilde{\boldsymbol{w}}$ is the modified weighting function added by the streamline upwind contribution. The expression for the modified weighting function is as follows:

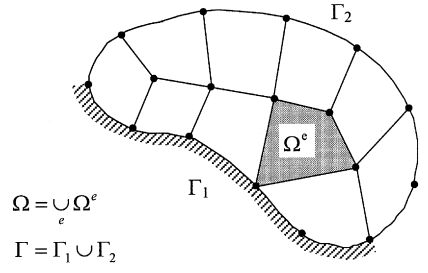

Fig. 1. Finite element discretization of the calculation domain Ω.

$$\tilde{w} = w + \frac{zh_e}{2|u_e|} u_j^e w_{,j}, \tag{9a}$$

$$z = \coth(\alpha) - 1/\alpha, \tag{9b}$$

$$\alpha = \frac{|u_e| h_e}{2v}, \tag{9c}$$

where u_e is the velocity at element center, h_e the element characteristic length, and α is the element Reynolds number.

In this work, the problem was defined in two-dimensional geometry. For mumerical calculation, a four node element was used to apply VOF method efficiently. Integrals in Eq. (8) were evaluated by Gauss quadrature. In order to prevent "locking" due to over-constraint, a reduced integration (Hughes et al., 1979; Reddy and Gartling, 1994; Carey and Oden, 1986) was used to evaluate the integrals of the penalty term. The iterations were terminated when the absolute error from previous iteration became smaller than the given tolerance ($|u_i - \hat{u}_i| < 10^{-6}$).

3. Selective VOF method

Most of the previous researches have adopted finite difference method or finite volume method to solve the aforementioned problem. Finite difference scheme is known to have difficulties in mesh generation when the computational domain is complex. For problems having complicated domain, finite element method (FEM) may be a more appropriate technique due to its simplicity in mesh generation. In this work, modified VOF method compatible with FEM was employed to analyze the flow problem with moving free surface.

In VOF method, Eq. (1) for the volume fraction F is solved simultaneously with other governing equations. Fig. 2 shows a typical pattern of the free surface when the fluid fills a mold cavity. Depending on the value of the volume fraction F in an element, the whole domain is divided into three categories by the following criterion:

$$F(\boldsymbol{x}, t) = \frac{\text{volume of fluid}}{\text{volume of element}} = \begin{cases} 1 & \text{filled,} \\ > 0 \text{ and } < 1 & \text{partially filled,} \\ 0 & \text{empty.} \end{cases} \tag{10}$$

F is unity in the fluid region and zero in the region where the fluid is absent. Therefore, the free surface can be considered to exist in the partially filled elements with F values between zero and unity. This partially filled elements should form a region in which the free surface exists. In order to locate the free surface precisely, the number of elements involved in this region should be kept as small as possible. However, as Eq. (1) is solved numerically, the region becomes wider as time progresses due to false numerical diffusion of F (Hirt and Nichols, 1981). In order to prevent this numerical smearing of the free surface, a special treatment is needed.

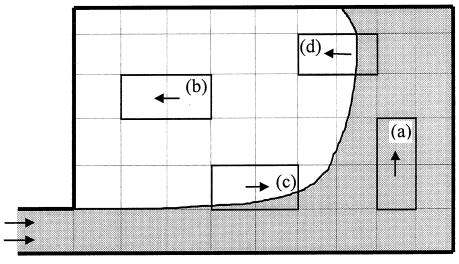

Fig. 2. Illustration of the flow front orientation.

Donor–acceptor scheme (Hirt and Nichols, 1981) is a popular method for overcoming such smearing of the free surface. Other methods, such as SLIC (Noh and Woodward, 1976), Youngs' scheme (Youngs, 1982), FLAIR (Ashgriz and Poo, 1991; Mashayek and Ashgriz, 1995a; Mashayek and Ashgriz, 1995b), pattern filling technique (Jeong and Yang, 1995) and net inflow method (Wang and Wang, 1994) have been proposed. In spite of the differences in the detail, the basic concept in each method is similar in that the free surface is numerically reconstructed by considering the slope of the free surface to prevent the smearing. Instead of solving Eq. (1) directly, volume flux across the element boundary is estimated and the change in F of the element is monitored.

Integration of the equation of volume fraction (Eq. (1)) for each element and discretization by the explicit scheme gives (Hirt and Nichols, 1981; Nichols et al., 1980; Partom, 1987)

$$F_i^{\text{new}} = F_i^{\text{old}} + \frac{\Delta t}{\int_{\Omega_i} d\Omega} \times \left[- \int_{\Gamma_i} (F_\Gamma \boldsymbol{u} \cdot \boldsymbol{n}) \, d\Gamma \right], \tag{11}$$

where F_i^{old} and F_i^{new} are the volume fractions of fluid in element i at previous and present times, Δt the calculation time step and Γ_i is the boundary of the element. The last term in Eq. (11) represents the increase of F due to incoming volume flux. F_Γ is the value of F on the boundary defined as

$$F_{\Gamma_{ik}} = \frac{\text{fluid volume transferred}}{\text{total volume transferred through } \Gamma_{ik}}, \tag{12}$$

where subscript i indicates the ith element and subscript k denotes the kth boundary of the ith element. F_Γ is a parameter which depends on the orientation of the free surface. Once F_Γ is known, the integral in Eq. (11), which represents the net flux of F into the element i, can be evaluated to give the net flux of F into the element i. F values after time increment Δt can then be updated and the free surface location can be determined. Therefore, the problem is simplified down to determination of the value of F_Γ.

In this work, an algorithm using four node element is proposed to determine the volume flux across the boundary F_Γ. The proposed scheme uses the concept of donor and acceptor elements as in the donor–acceptor scheme, but is modified to make compatible with FEM having irregular meshes. In order to determine the values of F_Γ, typical cases that could appear between two adjacent elements are considered as in Fig. 2. In case (a) of Fig. 2, two adjacent elements are in the fluid region, and the volume flux of fluid is $\int_{\Gamma_i} (\boldsymbol{u} \cdot \boldsymbol{n}) \, d\Gamma$ ($F_\Gamma = 1$). In case (b) of Fig. 2, two adjacent elements are outside the region of fluid, and there is no fluid in the elements. Thus the volume flux across the boundary is 0 ($F_\Gamma = 0$). Unlike the previous cases, in the cases (c) and (d) of Fig. 2, the value of F_Γ is not evident. Comparing the cases (c) and (d) of Fig. 2, it is apparent that the values of volume flux across the element boundary are different. This suggests that the volume flux across the boundary F_Γ is affected not only by the volume fraction but also by the orientation of the free surface. The information about the orientation in the element is provided by volume fractions of the element and the neighboring elements. In this study, the free surface was divided into two types by its orientation. The value of F_Γ was determined according to the orientation of the free surface.

In Fig. 3, some typical configurations in the free surface region are shown. Neighboring elements are classified as either donor or acceptor by the sign of the velocity. Upstream element is defined as the donor, and downstream element as the acceptor. In the proposed method, the value of F_Γ is taken

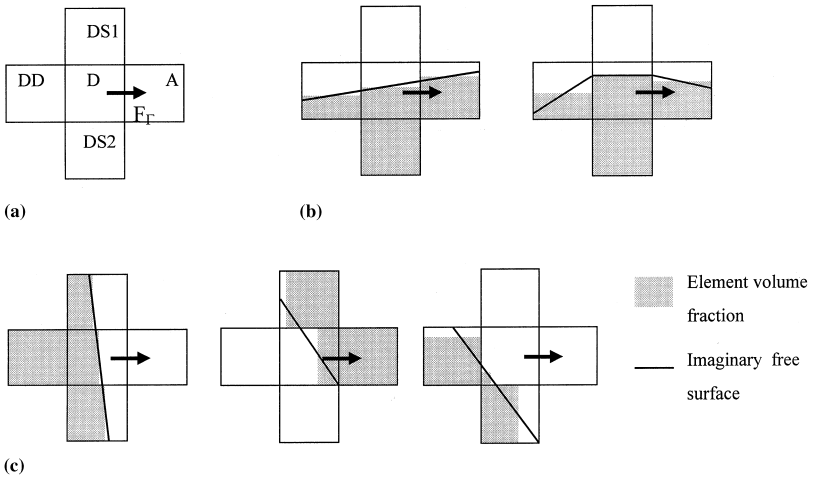

Fig. 3. Determination of F_Γ between donor and acceptor elements: (a) definition for donor and acceptor elements, (b) cases when $F_\Gamma = F_D$, and (c) cases when $F_\Gamma = F_A$.

from the volume fraction of either the donor or the acceptor depending on the orientation of the free surface.

If the free surface lies approximately in the perpendicular direction to the element boundary between the donor and the acceptor, the volume fraction of the donor is used as the value of F_Γ. If the surface lies in parallel or lies inclined by some degree, for example 45°, F_Γ is taken as the volume fraction of the acceptor. There are a number of cases according to the variations in the orientations of the free surface. These cases can be summarized and represented by the following algorithm:

if $(F_D = 1$ or $F_D = 0)$ then $F_\Gamma = F_D$
else
  if $((F_{DD} = 1$ and $F_A = 0)$ or $(F_{DD} = 0$ and $F_A = 1)$ then $F_\Gamma = F_A$
  else if $((F_{DD} = F_A = 1)$ or $(F_{DD} = F_A = 0))$ then $F_\Gamma = F_D$
  else if $(F_A = 1)$ then $F_\Gamma = F_A$
  else if $((0 < F_{DD}, F_A < 1)$ and $(F_{DS1} = 1$ and $F_{DS2} = 0))$ then $F_\Gamma = F_D$
  else if $(F_{DD} > F_D > F_A$ or $F_{DD} < F_D < F_A)$ then $F_\Gamma = F_A$
  else $F_\Gamma = F_D$
end if

Here F_D and F_A are the volume fractions of the donor and the acceptor, respectively. F_{DD} is the volume fraction of the neighboring element of the donor placed opposite to the acceptor. F_{DS1} and F_{DS2} are the volume fractions of the other neighboring elements of the donor (see Fig. 3).

The problem is simplified to choosing the volume fraction of donor or acceptor for determination of the value for F_Γ. Therefore, this algorithm can generally be applied to irregular mesh systems without additional calculations and can be extended to three-dimensional problems without great difficulties. If the boundary of an element coincides with a wall or a line of symmetry, there is no adjacent element on the corresponding side. In this case, an imaginary element is assigned as shown in Fig. 4. The volume fraction of the imaginary element is defined as 1, 0, or F_D according to the orientation already determined by the actual adjacent elements. The algorithm can then be applied in the same manner.

Since the net influx into an element is obtained by the procedure described above, the new volume fraction can be calculated once the calculation time step is given. However, if the calculation time step is fixed a priori, it is possible for an element to be excessively filled or emptied, i.e., the volume fraction can become greater than unity or less than 0 after a given time step. Therefore, in order to prevent this, the calculation time step Δt must satisfy the following constraints (see Eq. (11)):

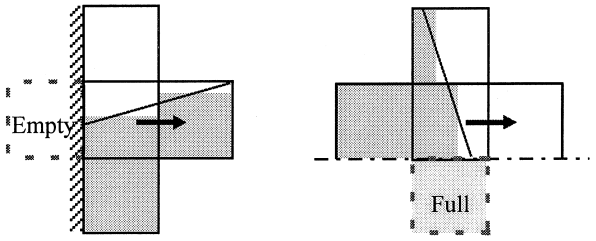

Fig. 4. Illustration of imaginary elements for wall or symmetric boundaries.

If volume flux into the element > 0:

$$\Delta t \leqslant \frac{\left(1 - F_i^{\text{old}}\right) \int_{\Omega_i} \mathrm{d}\Omega}{-\int_\Gamma (F_\Gamma \boldsymbol{u} \cdot \boldsymbol{n})\, \mathrm{d}\Gamma}. \tag{13a}$$

If volume flux into the element < 0:

$$\Delta t \leqslant \frac{\left(0 - F_i^{\text{old}}\right) \int_{\Omega_i} \mathrm{d}\Omega}{-\int_\Gamma (F_\Gamma \boldsymbol{u} \cdot \boldsymbol{n})\, \mathrm{d}\Gamma}. \tag{13b}$$

Here $-\int_\Gamma (F_\Gamma \boldsymbol{u} \cdot \boldsymbol{n})\, \mathrm{d}\Gamma$ is the volume flux into the element. $\left(1 - F_i^{\text{old}}\right) \int_{\Omega_i} \mathrm{d}\Omega$ and $\left(0 - F_i^{\text{old}}\right) \int_{\Omega_i} \mathrm{d}\Omega$ represent the available volume occupied by fluid in the element. The time step should be selected so as to satisfy the above limitations simultaneously for all the elements. The value of time step thus obtained satisfies Courant condition ($u_i \Delta t / \Delta x_i = 1$) automatically for the explicit time difference.

The overall numerical procedure is summarized as follows:

(1) Divide the whole domain into meshes.
(2) Solve the governing equations of flow by FEM.
(3) Determine the value of F_Γ at each boundary of the element by considering the free surface orientation.
(4) Calculate the volume flux into the element.
(5) Determine the calculation time step and obtain the volume fraction at the new time.
(6) Define the calculation domain using the updated volume fractions of the elements.
(7) Repeat steps (2)–(6) until the final time is reached.

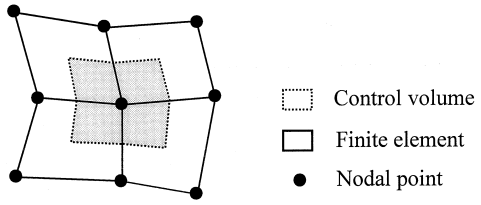

Fig. 5. Definition of a control volume.

When solving the governing equations, the volume fraction of an element is used. However, in order to represent the flow front, it is convenient to use the nodal values. A control volume which consists of sub-elements as shown in Fig. 5 was constructed and the volume fraction of the control volume was taken as the average of the volume fractions of surrounding elements

$$F^i_{CV} = \frac{\sum F^i_k V^i_k}{\sum V^i_k}, \tag{14}$$

where subscript i denotes the ith control volume and subscript k indicates a sub-element in a control volume. V^i_k is the volume of the sub-element, and F^i_k is the volume fraction. Each volume fraction of a control volume corresponds to a node, and the shape of the free surface is represented by contour lines along which the value of volume fractions is 0.5.

In this study, rule of mixture was used to estimate the properties of the partially filled element. The empty elements were assumed to be occupied by air. The density and the viscosity of air were given as 1 kg/m^3 and 10^{-5} Pa s, respectively. Stress free conditions for normal and tangential directions of the free surface were applied as the boundary conditions.

4. Verifications of the scheme

In order to verify the proposed scheme, two problems were analyzed, namely, broken dam problem and solitary wave propagation problem. The numerical results were compared with available data from the previous works.

In the broken dam problem, as shown in Fig. 6(a), a fluid column collapses under gravitation as the containing dam is removed suddenly. Initial domain is simple and both advancing and receding motions of the free surface exist at the same time. Moreover, numerical as well as experimental data are available for verification of the results. Martin and Moyce (1952) did experiments while Halrow and Welch (1965), Hirt and Nichols (1981), Huerta and Liu (1988) and Wang and Wang (1994) performed numerical studies.

In order to compare with the experimental data by Martin and Moyce (1952), the fluid was taken as water ($\rho = 1000$ kg/m^3, $\mu = 10^{-3}$ Pa s). The initial shape of the fluid column was a square ($H = 0.05715$ m). The Reynolds number based on the characteristic velocity $\sqrt{2gH}$ and the characteristic length H was 6.04×10^4. The accuracy of the free surface prediction depends on the calculation mesh in the fixed grid system. To test the dependency on the mesh system, four types of meshes were used. The number of elements were set to be either 264 (24×11) or 735 (35×21). Both uniform and non-uniform meshes were used in each case. The calculated mesh in the case of 735 non-uniform elements is shown in Fig. 6(b). The velocity vectors and flow patterns at various times for 735 non-uniform meshes are presented in Fig. 7. For the convenience of comparison with the experimental results, dimensionless time and water front location along the bottom are defined as $t^* = t\sqrt{g/H}$ and $x^* = x/H$,

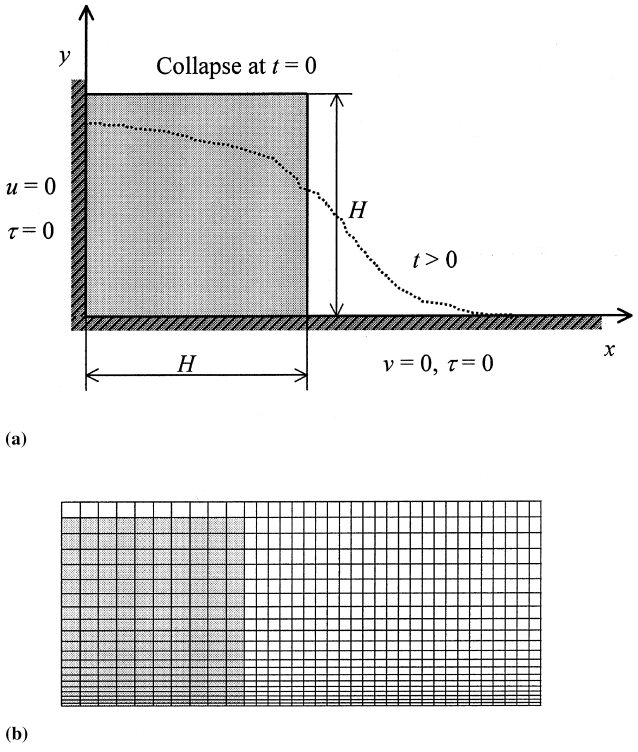

Fig. 6. Definition sketch (a) and finite element mesh (b) used in the analysis of the broken dam problem (35×21 non-uniform mesh).

respectively. As shown in Fig. 8, calculation results show good agreement with the experimental data. Better results can be obtained when more number of meshes are used. For coarse meshes, solution accuracy can be enhanced if the meshes are refined near the bottom where large variation of the free surface occurs.

The second verification problem was the solitary wave propagation. In this problem, a solitary wave travels back and forth in a container with a finite span (see Fig. 9(a)). Laitone (1960) and Byatt-Smith (1971) obtained analytic solutions for inviscid fluid in infinite domain. Experimental works were done by Maxworthy (1976) and Chan and Street (1970). Numerical studies were also performed by Ramaswamy and Kawahara (1987), Choi (1996), Baek and Chung (1996) and Kim (1998). As shown in Fig. 9(b), the computational mesh was a regular array except in the central region where the elements were slightly deformed according to the initial shape of the wave. Again the fluid was taken as water. The domain was finite and the depth and the length of the domain were set to be 1 and 16 m, respectively. The Reynolds number based on the characteristic velocity $\sqrt{gd}H/d$ and the characteristic length $H = 0.2$ m was 1.25×10^5. Slip boundary conditions were given at the wall. The initial conditions were specified as in the work of Laitone (1960):

$$u = (gd)^{0.5}\frac{H}{d}\operatorname{sech}^2\left[\left(\frac{3H}{4d^3}\right)^{0.5}x\right], \tag{15a}$$

$$v = (3gd)^{0.5}\left(\frac{H}{d}\right)^{1.5}\left(\frac{y}{d}\right)\operatorname{sech}^2\left[\left(\frac{3H}{4d^3}\right)^{0.5}x\right]\tanh\left[\left(\frac{3H}{4d^3}\right)^{0.5}x\right], \tag{15b}$$

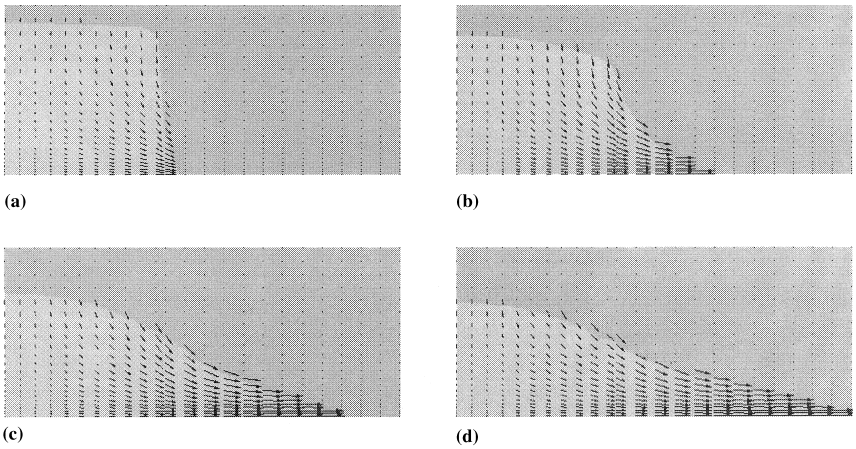

Fig. 7. Velocity vectors and free surface positions at different times for the broken dam problem. Results of numerical calculation with 35×71 uniform mesh: (a) 0.02971 s, (b) 0.05969 s, (c) 0.09011 s, and (d) 0.1105 s.

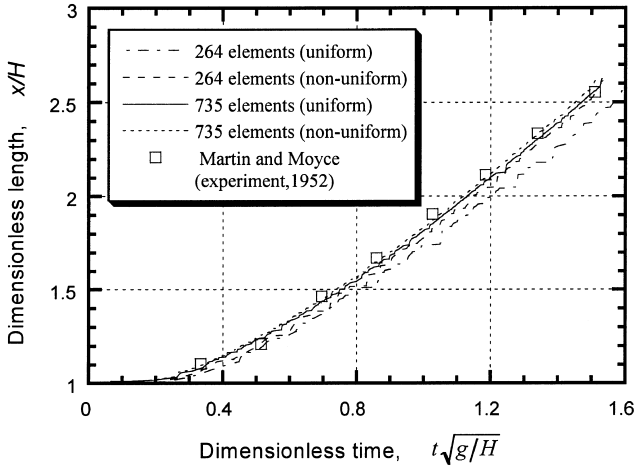

Fig. 8. Comparison of front tip position by numerical calculation with experimental result.

$$y = d + \eta = d + H\,\mathrm{sech}^2\left[\left(\frac{3H}{4d^3}\right)^{0.5} x\right]. \tag{15c}$$

In this study, the ratio between the water depth and the wave height H/d was varied from 0.2 to 0.5. Fig. 10 shows the flow patterns and velocity vectors during one period when $H/d = 0.4$. At a quarter or three quarters of a period, the wave height reaches a maximum as the wave runs up the wall and kinetic energy of the wave is converted into potential energy. Analytical solution is available for infinite domain with finite depth. Average velocity of the wave c and the pressure P can be obtained analytically as (Laitone, 1960):

$$\frac{c}{(gd)^{0.5}} = 1 + \frac{1}{2}\frac{H}{d} + \mathrm{O}\left(\frac{H}{d}\right)^2, \tag{16a}$$

$$P = \rho g(d + h - y) + \mathrm{O}\left(\frac{H}{d}\right)^2. \tag{16b}$$

Fig. 11 shows the calculated pressure distributions at various times. The results show close agreement with the analytic solution as given in Eqs. (16a) and (16b). The quarter of a period when the wave reaches the highest run-up along the right side wall can be calculated using the average wave velocity as given in Eq. (16a). As shown in Fig. 12, the calculated values are slightly larger than those from analytic solutions. The reason is that the analytic solution was worked out for infinite domain, while the numerical solution was obtained for a finite domain with side walls. In the finite domain, because the wave crest stays for a while at the side wall, the spatial phase shift appears (Maxworthy, 1976). Therefore, the times for the maximum run-up height are larger than those from analytic solution (Ramaswamy and Kawahara, 1987; Baek and Chung, 1996; Kim, 1998).

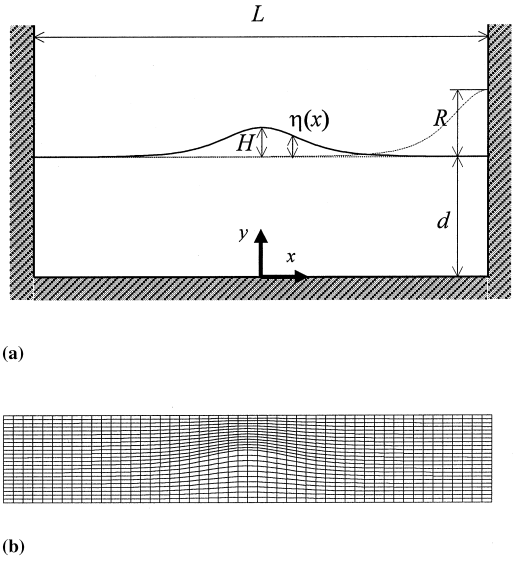

Fig. 9. Definition sketch and finite element mesh used in the solitary wave propagation problem: (a) definition sketch, and (b) finite element mesh.

Byatt-Smith (1971) obtained the maximum run-up height analytically by the method of superposition

$$\frac{R_{\max}}{d} = 2\left(\frac{H}{d}\right) + \frac{1}{2}\left(\frac{H}{d}\right)^2 + \mathrm{O}\left(\frac{H}{d}\right)^3. \tag{17}$$

Fig. 13 shows the comparison of the numerical results with the analytic solution of Byatt-Smith (1971), experimental data by Maxworthy (1976), Chan and Street (1970), and the nu-

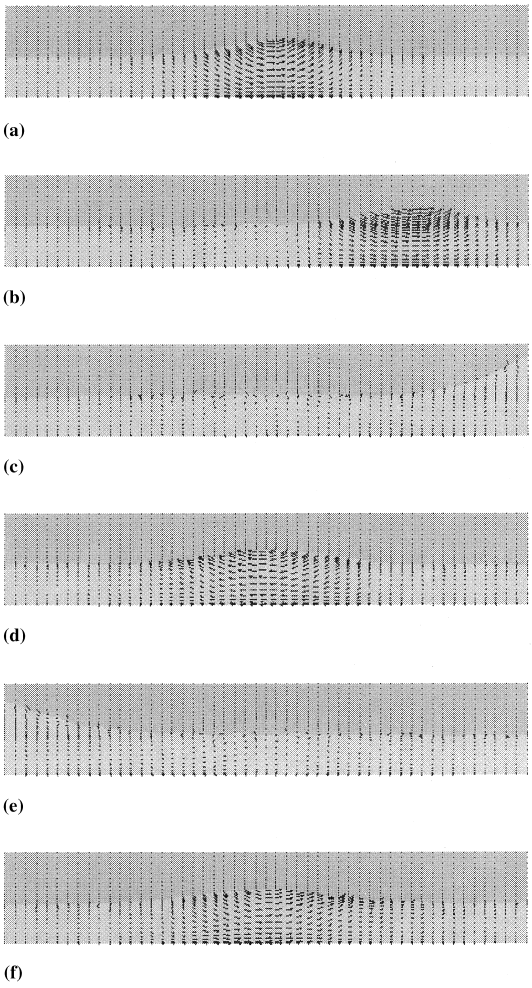

Fig. 10. Velocity vectors and free surface positions at different times for the solitary wave propagation problem. Numerical results for $H/d = 0.4$: (a) 0.000 s, (b) 1.151 s, (c) 2.313 s, (d) 4.523 s, (e) 6.916 s, and (f) 9.134 s.

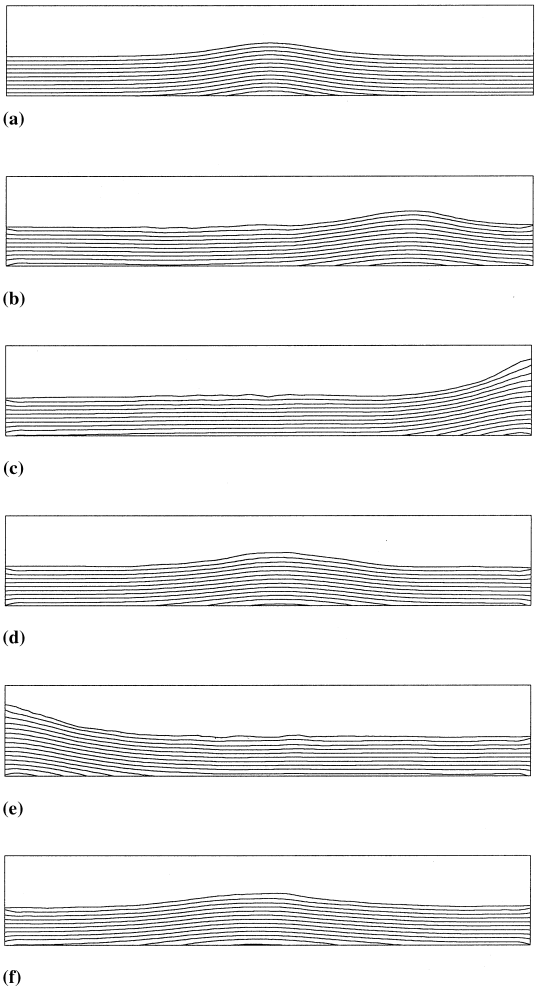

Fig. 11. Pressure contours at different times for the solitary wave propagation problem. Numerical results for $H/d = 0.4$: (a) 0.000 s, (b) 1.151 s, (c) 2.313 s, (d) 4.523 s, (e) 6.916 s, and (f) 9.134 s.

merical results of Choi (1996). As can be seen, good agreements were observed.

It is noted that the Reynolds numbers for the examples in this section are relatively high. This is due to the characteristic lengths taken for the Reynolds numbers. These high Reynolds numbers did not pose any difficulty in the numerical calculation even without employing a turbulence model.

5. Numerical examples

In order to illustrate the possibility of application to more complicated problems, mold filling processes were analyzed. Three cases were considered with a mold with rectangular cross-section:

Case 1. 2D planar and horizontal flow (without gravity).

Case 2. 2D planar and vertical flow (with gravity along the axis of symmetry).

Case 3. Axisymmetric and vertical flow (with gravity along the axis of symmetry).

The computational mesh and boundary conditions were given as Fig. 14. The average inlet velocity was given as 1 m/s and a half width of the inlet was 0.1 m. The density was 1000 kg/m^3 and the fluid viscosity was taken as 1 Pa s. The

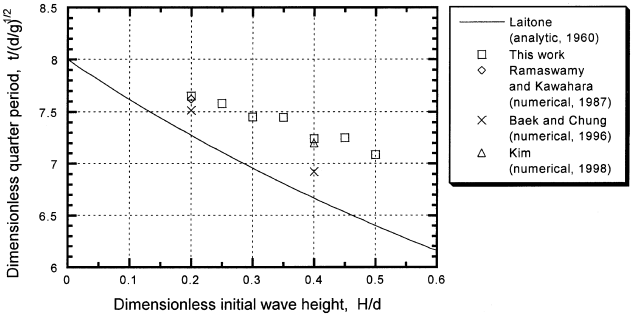

Fig. 12. Comparison of the quarter of a period by numerical method with previous numerical and analytic solutions for different initial wave heights.

Reynolds number based on the inlet velocity and the inlet width was 200. Figs. 15–17 show the flow patterns and velocity vectors at various times for each case.

As the results of Case 1 show, the fluid enters straightly forward in the beginning of filling. When the fluid encounters the wall, it changes direction and flows along the wall until it meets the inlet flow. The free surface then forms a closed curve

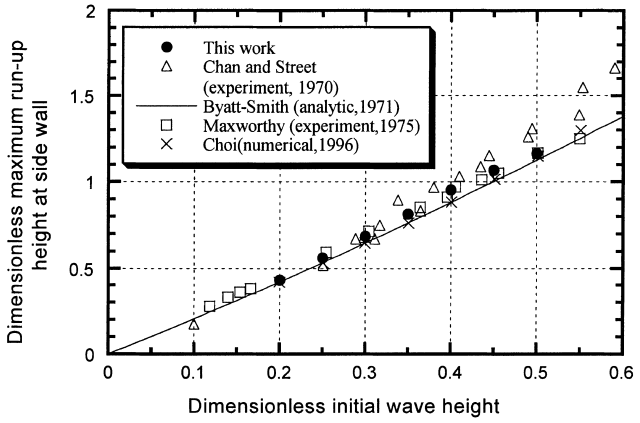

Fig. 13. Dimensionless maximum run-up heights as functions of dimensionless initial wave height. Comparison between the numerical results with existing data.

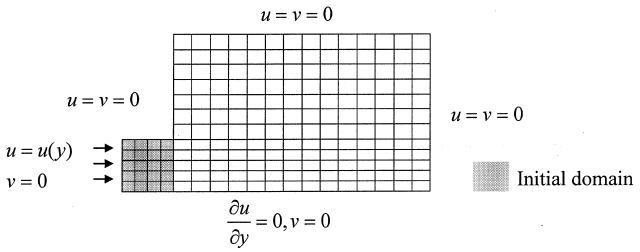

Fig. 14. Finite element mesh and boundary conditions for the mold filling problem.

in the central region. In other cases, the fluid accumulates from the bottom of the mold in a sequential manner due to the gravity effect. As shown in the results of Case 2, the flow is similar to Case 1 in the beginning of filling. However, the recirculant fluid column collapses toward the bottom as the gravity effect becomes dominant. After this, the free surface rises horizontally until filling is completed. In Case 3, the fluid column collapses earlier than Case 2. This effect is due to the

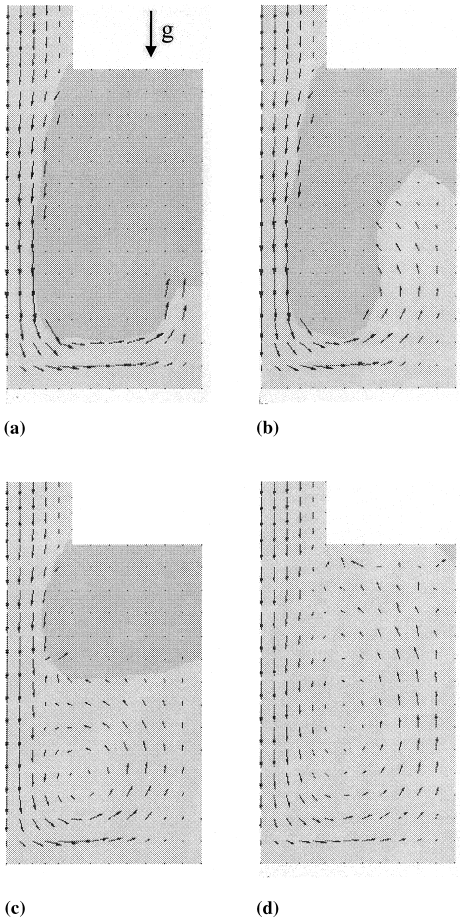

Fig. 16. Velocity vectors and free surface positions at different times for the mold filling of a horizontal mold in the presence of gravity at different times (Case 2): (a) 0.4999 s, (b) 0.7509 s, (c) 0.9991 s, and (d) 1.485 s.

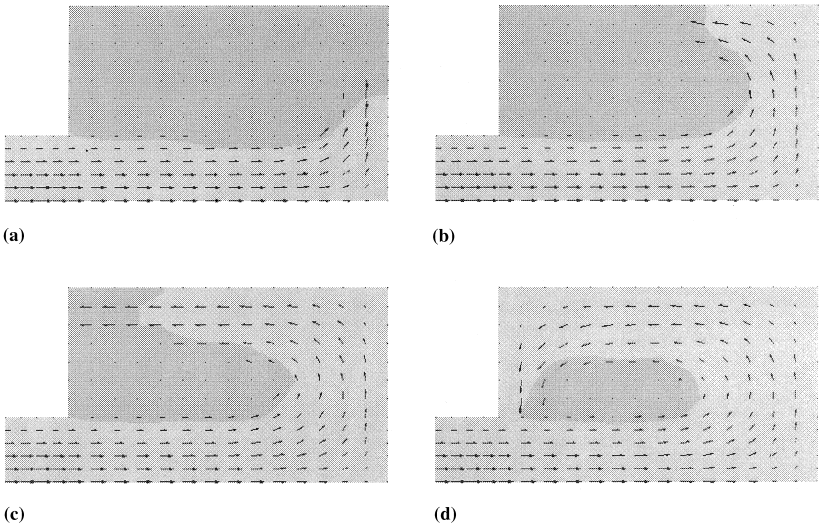

Fig. 15. Velocity vectors and free surface positions at different times for the mold filling problem of a horizontal mold (Case 1). No gravity effect was considered: (a) 0.4996 s, (b) 0.7505 s, (c) 0.9994 s, and (d) 1.248 s.

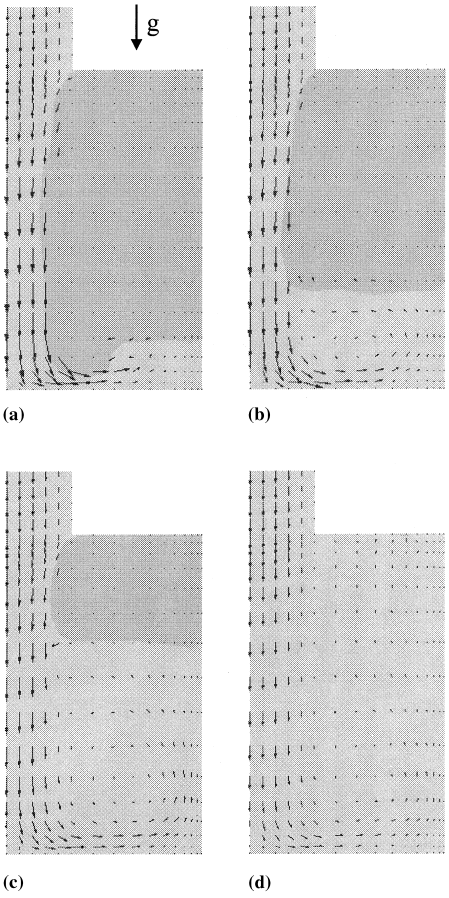

Fig. 17. Velocity vectors and free surface positions at different times for the mold filling of a vertical axisymmetric mold in the presence of gravity: (a) 0.9981 s, (b) 2.003 s, (c) 3.999 s, and (d) 5.899 s.

decreasing velocity near the side wall as the volumes of elements are increased proportionally with distance from the central axis in axisymmetric flow.

In order to verify the accuracy of the numerical scheme, fill times were compared. As the inlet velocity was given, the fill times were obtained as 1.5 s for Cases 1 and 2 and 6.0 s for Case 3. In the numerical analyses, the fill times were calculated as 1.506, 1.524 and 5.944 s, respectively, for each case. As can be seen, the errors are less than 2%. This further verifies that the current scheme satisfies the mass conservation closely. The proposed numerical scheme can predict the moving free surface correctly without loss or addition of fluid according to the accumulated errors during calculation.

6. Concluding remarks

A numerical method has been developed to simulate the incompressible, viscous flow with moving free surface. In order to represent the locations of the moving free surface, VOF method was adopted. To prevent the numerical diffusion, a selective VOF method was proposed to determine the volume flux of fluid between adjacent elements. This scheme is based on the concept of donor and acceptor and is compatible with a irregular mesh and can be extended to 3D geometry.

The proposed method was verified by comparing the results with previous researches, and has been applied to the simulation of mold filling as an engineering application. In the calculation of verification problems, the results showed good agreements. Due to the effective use of VOF method which is free from difficulties in mesh generation, this method can be applied to analyze complicated problems such as mold filling process with free surfaces varying severely with time inside the mold cavity.

Acknowledgements

This work was supported by Korea Ministry of Education (ME94-A-03) and Turbo and Power Machinery Research Center at Seoul National University.

References

Ashgriz, N., Poo, J.Y., 1991. FLAIR: Flux line-segment model for advection and interface reconstruction. J. Comput. Phys. 93, 449–468.

Baek, J.H., Chung, H.Y., 1996. Numerical analysis of incompressible viscous fluid flow with free surface. CFD J. 5, 71–88.

Bellet, M., Chenot, J.L., 1993. A Lagrangian approach to fluid flow in metal casting processes. In: Wrobel, L.C., Brebbia, C.A. (Eds.), Computational Methods for Free and Moving Boundary Problems in Heat and Fluid Flow. Elsevier, London, pp. 287–316.

Brooks, A.N., Hughes, T.J.R., 1982. Streamline upwind/Petrov–Galerkin formulations for convection dominated flows with particular emphasis on the incompressible Navier–Stokes equation. Comput. Methods Appl. Mech. Engrg. 32, 199–259.

Byatt-Smith, J.G.B., 1971. An integral equation for unsteady surface waves and a comment on the Boussinesq equation. J. Fluid Mech. 49, 625–633.

Carey, G.F., Oden, J.T., 1986. Finite Elements, vol. VI. Prentice-Hall, Englewood Cliffs, NJ, USA.

Chan, R.K.-C., Street, R.L., 1970. A computer study of finite-amplitude water waves. J. Comput. Phys. 6, 68–94.

Choi, H.G., 1996. A study on segregated finite element algorithms for the Navier–Stokes equations. Ph.D. Thesis, Seoul National University.

Dhatt, G., Gao, D.M., Cheikh, A.B., 1990. A finite element simulation of metal flow in moulds. Int. J. Numer. Methods Engrg. 30, 821–831.

Floryan, J.M., Rasmussen, H., 1989. Numerical methods for viscous flows with moving boundaries. Appl. Mech. Rev. 42, 323–341.

Harlow, F.H., Welch, J.E., 1965. Numerical calculation of time-dependent viscous incompressible flow of fluid with free surface. Phys. Fluids 8, 2182–2189.

Hirt, C.W., Nichols, B.D., 1981. Volume of fluid (VOF) method for the dynamics of free boundaries. J. Comput. Phys. 39, 201–225.

Huerta, A., Liu, W.K., 1988. Viscous flow with large free surface motion. Comput. Methods Appl. Mech. Engrg. 69, 277–324.

Hughes, T.J.R., Liu, W.K., Brooks, A., 1979. Finite element analysis of incompressible viscous flows by the penalty function formulation. J. Comput. Phys. 30, 1–60.

Jeong, J.H., Yang, D.Y., 1995. Numerical analysis of incompressible viscous flow with free surface using pattern filling and refined flow field regeneration technique. In: Proceedings of the KSME 1995 Fall Annual Meeting (I), pp. 903–908.

Kim, M.S., 1998. Finite element study of fluid flow with moving free surface. Ph.D. Thesis, Seoul National University.

Laitone, E.V., 1960. The second approximation to cnoidal and solitary waves. J. Fluid Mech. 9, 430–444.

Lewis, R.W., Usmani, A.S., Cross, J.T., 1995. Efficient mould filling simulation in castings by an explicit finite element method. Int. J. Numer. Methods Fluids 20, 493–506.

Lin, H.J., Hwang, W.-S., 1988. Combined fluid flow and heat transfer analysis for the filling of castings. AFS Trans. 96, 447–458.

Martin, J.C., Moyce, W.J., 1952. An experimental study of the collapse of liquid columns on a rigid horizontal plane. Philos. Trans. Ser. A 244, 312–324.

Mashayek, F., Ashgriz, N., 1995a. A hybrid finite-element-volume-of-fluid method for simulating free surface flows and interfaces. Int. J. Numer. Methods Fluids 20, 1363–1380.

Mashayek, F., Ashgriz, N., 1995b. Advection of axisymmetric interfaces by the volume-of-fluid method. Int. J. Numer. Methods Fluids 20, 1337–1361.

Maxworthy, T., 1976. Experiments on collisions between solitary waves. J. Fluid Mech. 76, 177–185.

Nichols, B.D., Hirt, C.W., Hotchkiss, R.S., 1980. SOLA-VOF: A solution algorithm for transient fluid flow with multiple free boundaries. Los Alamos Scientific Laboratory Report, LA-8355.

Noh, W.F., Woodward, P., 1976. SLIC (simple line interface calculation). In: van de Vooren, A.I., Zandbergen, P.J. (Eds.), Proceedings of the Fifth International Conference on Numerical Methods in Fluid Dynamics, Lecture Notes in Physics, vol. 59. Springer, New York, pp. 330–340.

Partom, I.S., 1987. Application of the VOF method to the sloshing of a fluid in a partially filled cylindrical container. Int. J. Numer. Methods Fluids 7, 535–550.

Ramaswamy, B., Kawahara, M., 1987. Arbitrary Lagrangian–Eulerian finite element method for unsteady, convective, incompressible viscous free surface fluid flow. Int. J. Numer. Methods Fluids 7, 1053–1075.

Reddy, J.N., Gartling, D.K., 1994. The Finite Element Method in Heat Transfer and Fluid Dynamics. CRC press, Boca Raton, USA.

Rice, A.B., 1993. Numerical simulation of mold filling processes. Ph.D. Thesis, Purdue University.

Swaminathan, C.R., Voller, V.R., 1994. A time-implicit filling algorithm. Appl. Math. Modelling 18, 101–108.

Tezduyar, T., Aliabadi, A., Behr, M., 1998. Enhanced-discretization interface-capturing technique (EDIT) for computation of unsteady flows with interfaces. Comput. Methods Appl. Mech. Engrg. 155, 235–248.

Usmani, A.S., Cross, J.T., Lewis, R.W., 1992. A finite element model for the simulation of mould filling in metal casting and the associated heat transfer. Int. J. Numer. Methods Engrg. 35, 787–806.

Viecelli, J.A., 1969. A method for including arbitrary external boundaries in the MAC incompressible fluid computing technique. J. Comput. Phys. 4, 543–551.

Wang, S.P., Wang, K.K., 1994. A net inflow method for incompressible viscous flow with moving free surface. Int. J. Numer. Methods Fluids 18, 669–694.

Youngs, D.L., 1982. Time-dependent multi-material flow with large fluid distortion. In: Morton, K.W., Baines, M.J. (Eds.), Numerical Methods for Fluid Dynamics. Academic Press, New York, pp. 273–285.